

## The Role of the Asian–Australian Monsoon System in the Onset Time of El Niño Events

JIANJUN XU AND JOHNNY C. L. CHAN

*Department of Physics and Materials Science, City University of Hong Kong, Hong Kong, China*

(Manuscript received 19 July 1999, in final form 3 April 2000)

### ABSTRACT

Based on the time of first occurrence of a significant sea surface temperature anomaly (SSTA) in the Niño-3.4 area (5°S–5°N, 170°–120°W), two types of El Niño episodes can be identified: the spring (SP) type in which the SSTA first increased to greater than 0.5°C in April or May, and the summer (SU) type in which this threshold is first reached in July or August. Composites of the SSTAs for these two types of events during the period 1950–97 show that the SP (SU) event is generally a stronger (weaker) warm episode in terms of the SSTA amplitude, and longer (shorter) in terms of the period during which the SSTA is greater than 0.5°C.

Before the occurrence of both types of El Niño episodes, the zonal wind anomalies over the western equatorial Pacific are always westerly. The east Asian winter monsoon is also strong. The difference between the two types is mainly in the timing of the occurrence of the westerly anomalies. For the SP (SU) events, these anomalies extend to the date line by January (May) of the El Niño year. A third component found in both types of El Niño episodes is anomalous southerlies over the northeastern coast of Australia during the El Niño year, which appear earlier in SP events. The difference between the two types of El Niño episodes is apparently phase locked to the annual variation in SST over the western equatorial Pacific.

A stronger east Asian winter monsoon and westerly anomalies in the previous summer are also found in some non-El Niño years. However, in these cases, no anomalous southerlies occur over the northeast of Australia. Therefore, it appears that only when anomalous northerlies from the east Asian winter monsoon converge with anomalous southerlies associated with the transition of Australian monsoon can sufficiently strong westerly anomalies form over the western equatorial Pacific to cause an El Niño event to occur. The presence of a strong south Asian summer monsoon in the previous year is also necessary. The timing of occurrence of southerlies over northeastern Australia apparently determines the onset time of an El Niño event.

### 1. Introduction

Many studies have shown that the Asian–Australian monsoon is linked to the interannual variability of the tropical ocean–atmosphere system, in particular the El Niño (EN) event (e.g., Shukla and Paolino 1983; Nicholls 1989; Li 1990; Tomita and Yasunari 1996; Ju and Slingo 1995; Soman and Slingo 1997). In fact, much scientific evidence now suggests that the Asian monsoon may strongly influence EN development (Yasunari 1990; Webster and Yang 1992; Lau and Yang 1996; Meehl 1997). Angell (1981) noted that sea surface temperature (SST) anomalies in the eastern equatorial Pacific (EEP) during fall and winter are highly correlated with the preceding Indian monsoon rainfall. Li (1990) and Xu et al. (1998a,b) reported that a strong east Asian winter monsoon favors an EN occurrence during the next half year. Holland (1986) found a positive corre-

lation between the onset date of the Australian summer monsoon and the EEP SST anomalies (SSTAs) in the months prior to onset, which therefore provides some predictive capability for the EN occurrence. On the other hand, many previous studies have stressed the role of EN in the interannual variability of the Indian monsoon. Nicholls (1984), for example, adopted SSTAs in the Indonesian–north Australian area as a predictor of the Indian monsoon rainfall. Rasmusson and Carpenter (1983) suggested that SSTAs in the eastern Pacific could be a potential predictor for the Indian monsoon rainfall. These previous works suggest that the Asian–Australian monsoon and the EN event form an intricately linked atmosphere–ocean interaction system.

A further complication in the relationship between this monsoon and the EN is the irregularity of EN events. For example, Rasmusson and Carpenter (1982) suggested that large-scale SSTAs first appear off the coast of Peru and then spread northwestward as well as westward along the equator into the central Pacific. But the 1982–83 warm event seemed to differ from this scenario in that the warming occurred first in the central equatorial Pacific (CEP) and then propagated eastward

---

*Corresponding author address:* Johnny Chan, Department of Physics and Materials Science, City University of Hong Kong, 83 Tat Chee Ave., Kowloon, Hong Kong, China.  
E-mail: johnny.chan@cityu.edu.hk

along the equator (Gill and Rasmusson 1983). This suggests that the basic EN evolution may have different types.

In fact, Quinn and Neal (1987) and Wang (1992) grouped past EN events into four levels according to the strength of the SSTA over the EEP. Classification of the EN can also be made with respect to the interval, as was done by Enfield and Cid (1991). Fu et al. (1986) categorized EN events into three types based on the zonal SST gradient pattern in the equatorial Pacific. Yasunari (1985) showed that major and minor EN events could be explained by the superposition of two dominant modes (2–30- and 40–60-month periods) detected in the interannual variability of the Walker circulation. Barnett (1991) advanced the idea of Yasunari (1985) to classify EN events into three categories according to the relation between the amplitude and phase of these two dominant periods. Lau and Sheu (1988) predicted two types of the EN cycle (2 and 4 yr) from a conceptual model. In addition, Wang (1995) pointed out substantial interdecadal variations of SST, and the onset of EN episodes are affected largely by the different climatic background of SST.

If the EN event is so closely linked to the Asia–Australian monsoon, some kind of seasonal phase locking should be expected since the latter has an obvious seasonal signal. Therefore, classifying EN events based on its onset time could offer some clue as to how the Asia–Australian monsoon may help trigger the EN event, which is the main objective of this study.

In section 2, the datasets used are described. The classification based on the time of occurrence of the EN event and the time evolutions of various parameters in each type are documented in sections 3 and 4, respectively. Section 5 examines the relationship between equatorial westerly anomalies and the various monsoon systems. How the Asian–Australian monsoon system may trigger El Niño events is discussed in section 6. All the results are then summarized in section 7.

## 2. Data

The present study utilizes data from four sources. Monthly mean global SST data on a  $2^\circ$  latitude  $\times$   $2^\circ$  longitude grid for the period 1950–97 are based on the analyses of Reynolds and Smith's (1994) Comprehensive Ocean–Atmosphere Data Sets. Monthly mean global zonal and meridional wind components for 1958–97 are from the National Centers for Environmental Prediction (NCEP)–National Center for Atmospheric Research reanalyses. The monthly Northern Hemisphere sea level pressure data on a resolution of  $5^\circ$  (latitude)  $\times$   $10^\circ$  (longitude) compiled by the U.K. Met. Office for 1950–97 are also used in this study. Missing values have been interpolated from the neighboring grid points. The pseudostress data over the Pacific Ocean on an  $84 \times 30$  grid during 1961–97 are from The Florida State University. Values of the monthly SST over the Niño-3,

Niño-3.4, Niño-4, and Niño-1+2 region (1950–97) are extracted from the homepage of the Climate Prediction Center (CPC). An optimum interpolation of ocean heat content (0/400m) data on a  $2^\circ$  latitude  $\times$   $5^\circ$  longitude grid for each month from January 1955 to December 1998 are obtained from the Scripps Institution of Oceanography. The decorrelation scales used are  $10^\circ$  zonally,  $5^\circ$  meridionally, and 3 months temporally, with a signal-to-noise ratio of 1. Small areas of missing data are filled by zonal linear interpolation. The grids were spatially smoothed in time with a 1–1–4–1–1 filter.

## 3. Classification of El Niño events

Many previous studies have discussed the onset of the warm event. For example, Rasmusson and Carpenter (1982) defined the onset phase to be the early stage of the warm episode when composite SSTAs along the Peruvian coast are near zero, but increasing rapidly. Philander (1985), on the other hand, suggested the period in spring as the onset phase.

To avoid confusing with the concept of onset phase in these studies, the first time when the SST over the CEP ( $5^\circ\text{S}$ – $5^\circ\text{N}$ ,  $170^\circ$ – $120^\circ\text{W}$ ) becomes significantly above normal (monthly mean of 1950–97) will be defined as the onset time of EN episodes. The Niño-3.4 SSTA showing the SST variation in the CEP appears to be a meaningful indicator for the EN event because this area has the largest equatorial east–west SST gradient (Wang 1995). Further, the anomalous warming here seems to be most influential to the shift of the rising branch of the Walker circulation and is highly correlated with the Southern Oscillation index. The Niño-3.4 SSTA is therefore chosen as the reference. The month when the SSTA first exceeded  $0.5^\circ\text{C}$  and persisted afterward is defined as the onset time of the EN event. It should be pointed out that this threshold of  $0.5^\circ\text{C}$  is also used by CPC in their definition of an EN event.

Twelve EN episodes (1951–52, 1957–58, 1963–64, 1965–66, 1968–69, 1972–73, 1976–77, 1982–83, 1986–87, 1991–92, 1994–95, 1997–98) occurred during 1950–98. Note that the 1953 and 1993 EN episodes were not included due to their short duration. The time evolution of the Niño-3.4 SSTA index during each of these episodes (Fig. 1) suggests that the onset time of EN event is either in spring (April or May) or summer (July or August). In other words, EN episodes can be defined into two types. One can be labeled as the spring (SP) onset type that includes 1957–58, 1965–66, 1972–73, 1982–83, 1991–92, 1997–98. These six episodes happen to coincide with the most significant EN events selected by Wang (1995) except for the 1986–87 episode. The other is the summer (SU) onset type that includes 1951–52, 1963–64, 1968–69, 1976–77, 1986–87, 1994–95.

To provide further confidence in such a classification, the SSTA indexes of three other regions (Niño-1+2, Niño-3, and Niño-4) are also examined in the same way

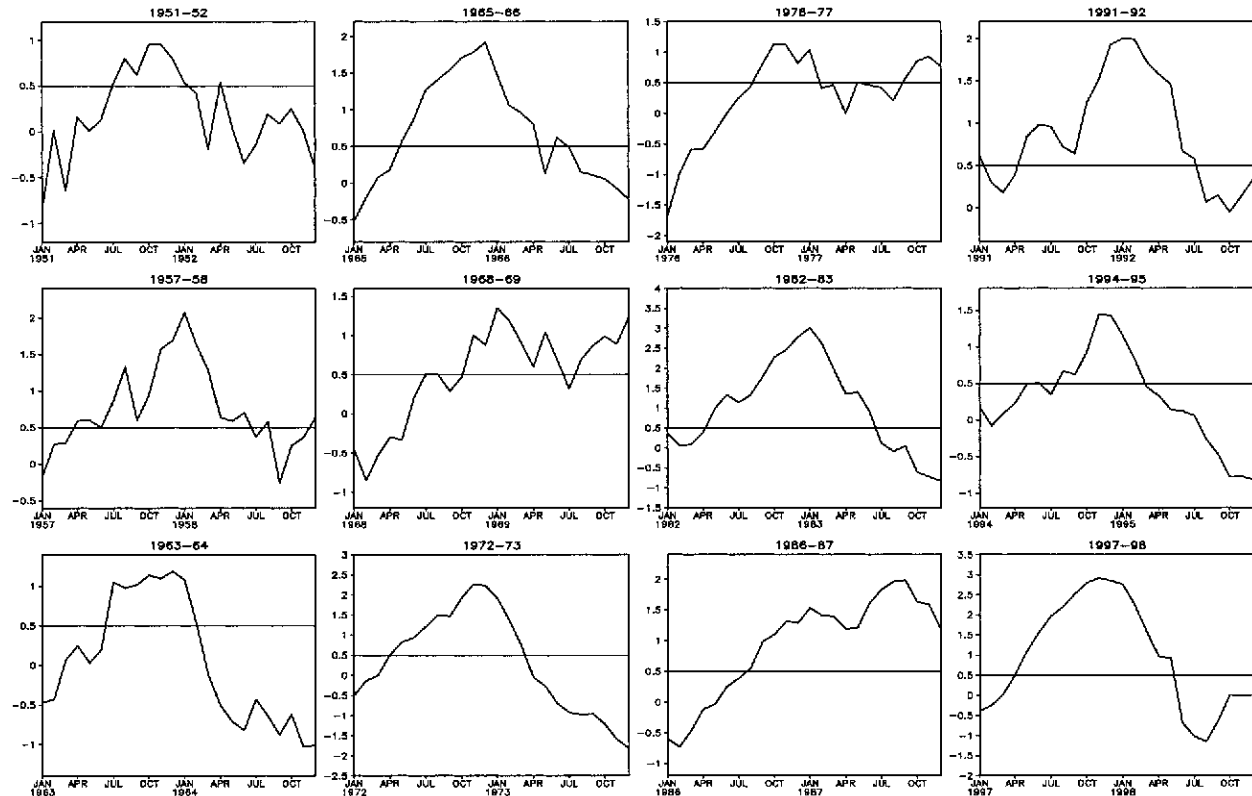


FIG. 1. Time series of the Niño-3.4 SSTA during the 12 EN episodes. The  $0.5^{\circ}\text{C}$  line is the threshold for identifying the onset time of the EN event.

to identify the time when the SSTA first rose above the threshold of  $0.5^{\circ}\text{C}$ . A comparison of the times of occurrence identified from the SSTA values of the different regions suggests that the classification is essentially the same (Table 1), perhaps with the exception of 1991.

#### 4. Comparison between the two types of episodes

##### a. SST time series

The composite Niño-3.4 SSTA time series of the two types of EN episodes (Fig. 2a) show that the SP type has a larger SSTA amplitude with a mean maximum SSTA of  $\sim 2.0^{\circ}\text{C}$  and a long duration (exceeding 14 months; when the  $\text{SSTA} > 0.5^{\circ}\text{C}$ ). All the six SP events in Fig. 1 lasted more than 12 months. In contrast, the SU type seems to be weaker with only a  $\sim 1.0^{\circ}\text{C}$  maximum anomaly, and is shorter in duration ( $\sim 8$  months). Five of the six SU episodes in Fig. 1 had a duration of less than 8 months. The 1986–87 episode had double peaks with the second one developing after the 1987 northern summer, but the onset time of the first stage is similar to the other five episodes. The other important feature is that the maximum anomaly in both types occurs in November–January, which implies that the mature phase of the EN event is highly phase locked with the seasonal cycle, irrespective of the onset time.

The phase locking can probably explain the difference in the maximum amplitude between the two types. The onset of the SP event occurs in April, which is the time when the SST is increasing over the western equatorial Pacific (WEP;  $5^{\circ}\text{S}$ – $5^{\circ}\text{N}$ ,  $130^{\circ}$ – $160^{\circ}\text{E}$ ; Fig. 2b). Thus, in the ensuing months, warmer water can propagate eastward, which results in a large SSTA amplitude observed in Fig. 2a. On the other hand, the SU event begins in July when the WEP SST starts to decrease (Fig. 2b).

TABLE 1. Onset time (see text for definition) of occurrence of the 12 EN episodes during 1950–97 based on four SSTA indexes over the eastern equatorial Pacific. For 1951, the time could not be determined based on the Niño-4 SSTA.

Year	Niño-3.4	Niño-1 + 2	Niño-3	Niño-4	Onset time
1951	Jul	May	Jul	—	Summer
1957	Apr	Feb	Apr	Apr	Spring
1963	Jul	Jul	Jul	Jul	Summer
1965	May	Apr	May	Jul	Spring
1968	Jul	Sep	Nov	Nov	Summer
1972	Apr	Feb	Apr	Apr	Spring
1976	Sep	May	Jun	Nov	Summer
1982	May	Jul	Apr	Apr	Spring
1986	Aug	Oct	Sep	Aug	Summer
1991	May	Nov	May	Mar	Spring
1994	Aug	Oct	Oct	Jun	Summer
1997	May	Mar	Apr	Apr	Spring

Therefore, the water that propagates eastward is slightly cooler. Further, since the maximum warming always occurs around December and January, less time is available to depress the thermocline. As a result, the maximum SSTA amplitude of SU events is generally smaller than that of SP events.

Note also from Fig. 2a that even though the onset times of the two types are different, the growth rate of the SSTA is essentially the same. This suggests that if the same mechanism is responsible for triggering the onset of the warm event, this mechanism must occur later in the SU type. This will be seen to be the case in the subsequent analyses. However, once the warm event starts, the processes that govern the evolution up to the peak in the SSTA should be very similar. On the other hand, the decay of the two types of events appears to be quite different. While the SSTA in the SP events quickly decreases to an appreciably negative value, that in the SU events hovers around zero for an extended period of time. Obviously, the physical mechanisms responsible for the decay of these two types of warm events should be different. The possible mechanisms will not be investigated in the present study, which focuses on the onset time. Results of such an investigation will be reported in the future.

#### b. Horizontal distribution of SST and wind stress anomalies

To reveal the differences between the spatial and temporal evolution of the two types of EN events, the SST and wind stress anomalies over the tropical Pacific ( $29^{\circ}\text{S}$ – $29^{\circ}\text{N}$ ,  $120^{\circ}\text{E}$ – $80^{\circ}\text{W}$ ) are composited for each type from January of the EN year (January 0) to July.

In January 0 of the SP event, the EEP is dominated by weak negative SST anomalies with a maximum value of around  $-0.3^{\circ}\text{C}$  while the western Pacific warm pool has a positive SST anomaly of  $\sim 0.2^{\circ}\text{C}$  (left-hand side of Fig. 3). Appreciable divergence occurs over the EEP corresponding to the negative SST anomaly. Over the WEP, weak westerly anomalies can be found that may have come from the equatorial Indian Ocean (EIO). Anomalous northerlies also prevail off the east Asian coast, which is associated with the stronger than normal east Asian winter monsoon.

In April 0, which is around the onset time of the SP event, two positive SSTA centers appear over the equatorial Pacific, one near the date line and the other off the Peruvian coast, the latter being stronger, which indicate the EN event onset. Wind stress anomalies become negligible over the EEP. However, prominent southerly anomalies appear off the northeastern coast of Australia, which may be related to the seasonal transition of Australian summer monsoon.

By July 0, positive SSTAs dominate over the entire EEP where strong convergence can be found, although the maximum anomaly is still off the Peruvian coast. Strong anomalous westerlies now prevail over the WEP.

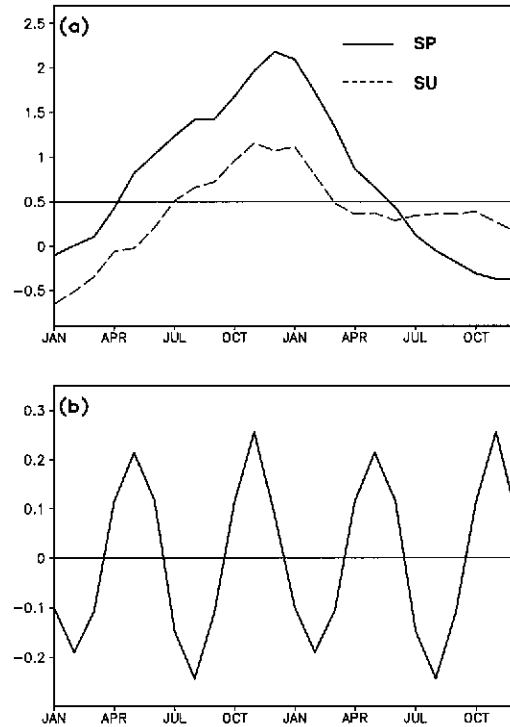


FIG. 2. (a) Composite time series of the SSTA over Niño-3.4 for the two types of EN episodes. Solid (dashed) line indicates the SSTA of the SP (SU) type. (b) Seasonal variation of SST relative to the annual mean over the WEP.

As compared with the SP event, the SU episodes show very different evolution characteristics (right-hand side of Fig. 3). In January 0, strong negative SSTAs with a negative maximum of over  $-1.0^{\circ}\text{C}$  dominate over the EEP. Anomalous easterlies prevail over the WEP. Similar to the SP event, the east Asian winter monsoon is also stronger than normal, as evidenced by the strong anomalous northerlies off the east Asian coast. By April 0, the maximum negative SSTA contracts to the Peruvian coast. Anomalous northerlies continue to prevail off the east Asian coast and anomalous westerlies begin to appear over the WEP. Off the northeast coast of Australia, weak anomalous northerlies are found instead of southerlies (as in the SP episodes). Notice, however, the similarity between the SU April 0 pattern and the SP January 0 pattern. It appears that the entire pattern is delayed for one season for the SU events.

In July 0, corresponding to the onset time of the SU episodes, the SST anomalies over the EEP are positive with two maximum anomaly centers located at  $\sim 150^{\circ}\text{W}$  and  $\sim 100^{\circ}\text{W}$ . Anomalous southerlies now appear off the northeast coast of Australia, which is similar to the feature in April 0 at the onset time of the SP events.

Thus, besides the westerly anomalies over the WEP, the northerly anomalies in the northern winter off the coast of east Asia and the southerly anomalies during the southern transition season off the northeast coast of

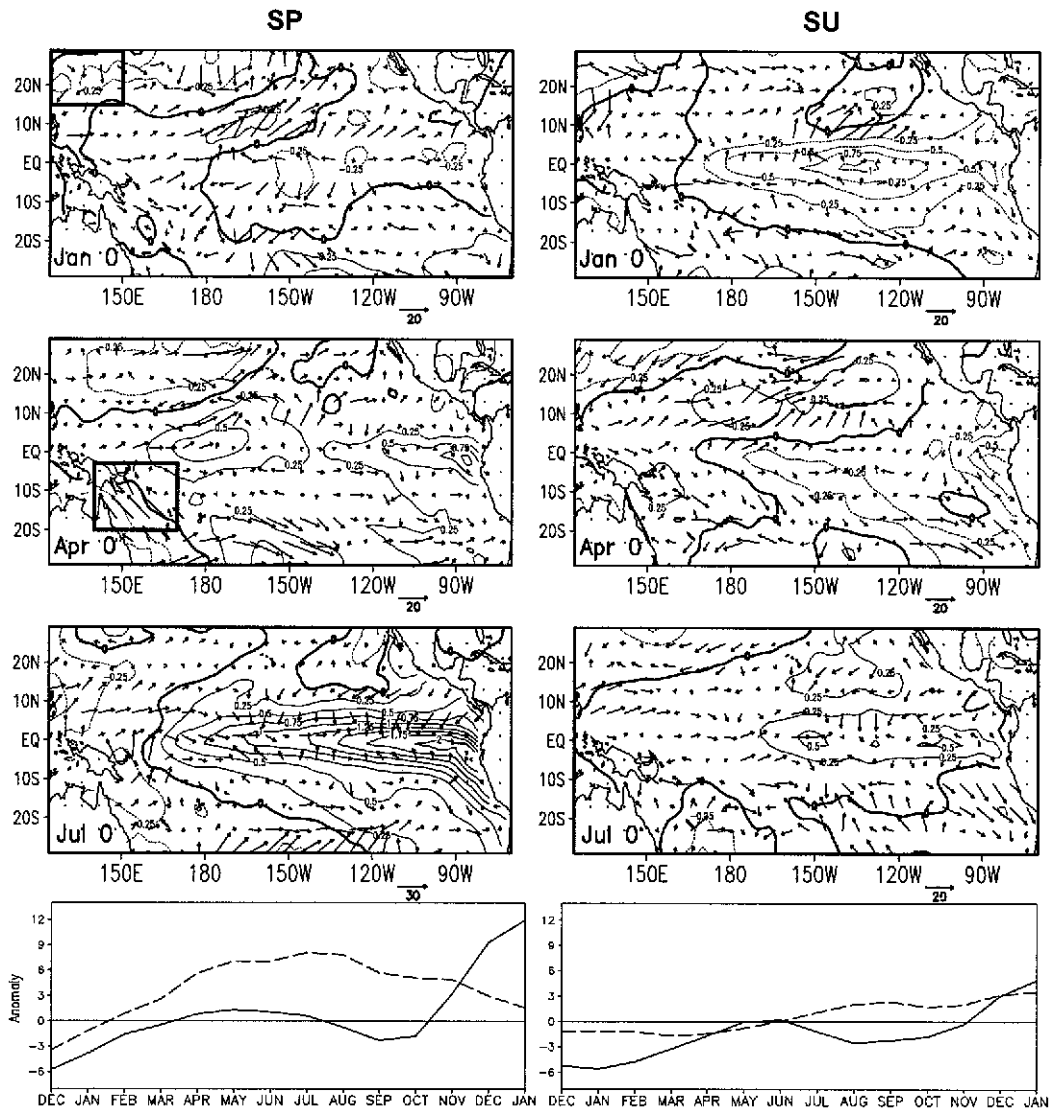


FIG. 3. Composites of SST and wind stress anomalies for (left) SP and (right) SU events from Jan to Jul of the EN year (Jan 0 to Jul 0). Only the months Jan 0, Apr 0, and Jul 0 are shown. Shaded areas indicate  $SSTA > 0.5^{\circ}\text{C}$ . The arrows indicate the vector wind stress anomalies. Note that the scale of the arrows (marked under the bottom of each panel) is not necessarily the same for all the panels. The bottom panel in each column shows time series of the mean meridional wind stress anomalies over the east Asian monsoon area ( $15^{\circ}\text{--}29^{\circ}\text{N}$ ,  $124^{\circ}\text{--}150^{\circ}\text{E}$ ; solid) and the Australian monsoon area ( $5^{\circ}\text{--}20^{\circ}\text{S}$ ,  $140^{\circ}\text{--}170^{\circ}\text{E}$ ; dashed), unit:  $(\text{m s}^{-1})^2$ . These two areas are indicated as boxes on the top left two panels.

Australia also have a close relationship with the onset of both types of EN episodes. To illustrate further the characteristics of the latter two features, the time series of meridional wind anomalies over two areas [ $15^{\circ}\text{--}29^{\circ}\text{N}$ ,  $124^{\circ}\text{--}150^{\circ}\text{E}$ , the east Asia winter monsoon (EAWM) area] and [ $5^{\circ}\text{--}20^{\circ}\text{S}$ ,  $140^{\circ}\text{--}170^{\circ}\text{E}$ , the Australian monsoon (AM) area] are examined (bottom of Fig. 3). For both types, northerly anomalies are quite appreciable over the EAWM area before the EN onset. However, the transition from northerly to southerly anomalies over the AM area occurs in February (June) for the SP (SU) event, which is about one to two months before the onset

time. Therefore, the time of occurrence of the transition from northerly to southerly anomalies over the AM area appears to be a key factor in determining the EN onset time, which is consistent with the finding of Holland (1986). A more detailed discussion will be made in the next section.

### c. SST time–longitude cross sections

To understand more clearly the differences in these two types of EN episodes, the time evolution of SSTAs over the equatorial Pacific ( $5^{\circ}\text{S}\text{--}5^{\circ}\text{N}$ ) are composited.

For the SP event (Fig. 4a), positive SSTAs with a maximum value of  $\sim 0.25^{\circ}\text{C}$  appear over WEP and the maritime continent in the summer prior to the EN year, and propagate slowly eastward. Around the onset time of the SP event, a positive anomaly of  $\sim 0.5^{\circ}\text{C}$  occurs along the Peruvian coast and then propagates westward and merges with the positive anomaly from the WEP. The positive SSTAs persist in the EEP for about 18 months. At the same time, the WEP is dominated by negative SSTAs with a maximum value of  $\sim 0.5^{\circ}\text{C}$ . Notice that positive SSTAs also exist over the EIO.

For the SU event, positive SSTAs begin to appear over the WEP around October of the year before the EN occurs (Fig. 4b), but are weaker than those in the SP event. Below-normal SSTAs persist over the CEP and EEP until spring of the EN year. After the onset time, the positive SSTAs over the EEP show a slow westward propagation. In addition, the east–west SST gradient is much weaker than that in the SP event.

#### d. Oceanic heat content anomalies from 0- to 400-m depth

In addition to SSTA, ENSO events are also associated with temperature anomalies below the ocean surface. To understand how these anomalies are related to the two types of EN events, the time evolution of subsurface heat content anomalies (HCAs) from 0- to 400-m depth is examined. In the summer of the year before a SP episode (from May  $-1$  to September  $-1$ ), positive HCAs are found in the WEP (Fig. 5a), part of which is contributed by the positive SSTA (see Fig. 4a). This corresponds to the accumulation of warm water near the western boundary prior to a warm event, as first suggested by Wyrtki (1975). The warm water starts to propagate eastward at around October  $-1$  at a speed far less than that of a typical Kelvin wave. This might correspond to the slow coupled air–sea mode discussed by Hirst (1986) and initiated through a reflection of Rossby waves off the western boundary (Battisti 1988; Suarez and Schopf 1988). A second maximum in HCA occurs around March 0 due to the enhancement of westerly anomalies (see Fig. 3), which is probably related to the Madden–Julian oscillation (MJO) activity over the WEP (to be discussed further in the next section). The warm water then continues to propagate eastward in step with the SSTA (see Fig. 4a).

For the SU episode, the conditions in the summer of year  $-1$  are similar as those in the SP case, with a maximum HCA in the WEP, though with a slightly weaker amplitude (Fig. 5b). However, this maximum generally remains stationary until around May or June before the entire HCA propagates eastward. The speed of propagation, however, is much faster than that in the SP episodes. The slow coupled air–sea mode also appears to be absent.

The results of Figs. 4 and 5 suggest the following. Accumulation of warm water over the WEP through a

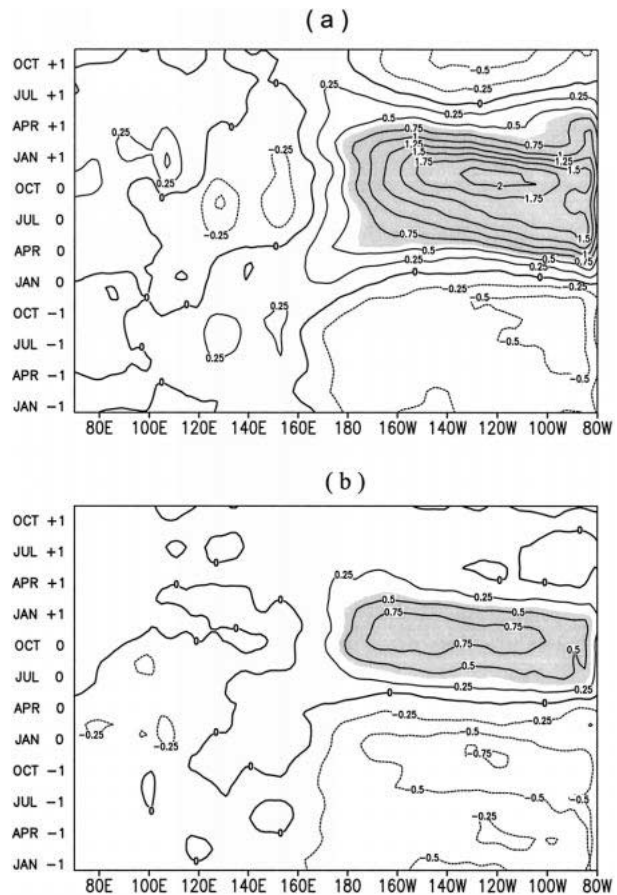


FIG. 4. Longitude–time section of SSTA composites over the equatorial area ( $5^{\circ}\text{S}$ – $5^{\circ}\text{N}$ ) for (a) SP and (b) SU. Shaded area indicates the SSTA  $> 0.5^{\circ}\text{C}$ .

deep layer occurs in both episodes during the summer of year  $-1$ . The eastward propagation of the warm water at the onset time also appears to be very similar. However, in the SP episodes, propagation of the subsurface water apparently begins much earlier than the onset time. This result further justifies separating the warm events into two categories.

The initiation of the Rossby waves in the SP episodes occurs near the tropical central North Pacific where an increase in the HCA begins at around July  $-1$  (Fig. 6a). Such a positive HCA then propagates westward and reaches the western boundary at around October  $-1$ . In the SU episodes, no such increase in the HCA is apparent (Fig. 6b).

#### e. Madden–Julian oscillation

The MJO has been suggested as an important contributor in the initiation of warm events (McPhaden 1999), since it tends to be most active during northern winter and spring (Slingo et al. 1999) and is associated with the westerly episodes originating over the Indian Ocean (Madden and Julian 1972, 1994). In order to

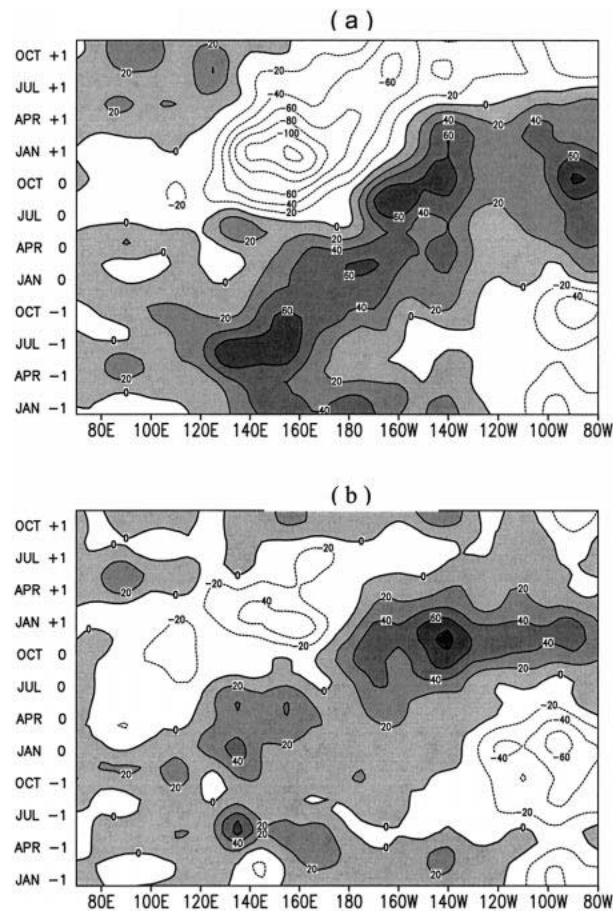


FIG. 5. Longitude–time section of HCAs from 0- to 400-m depth composites over the equatorial area ( $5^{\circ}\text{S}$ – $5^{\circ}\text{N}$ ) for (a) SP and (b) SU. Shaded areas indicate positive HCAs, unit:  $10^8 \text{ J m}^{-2}$ .

examine the contribution of the MJO, a bandpass filter (30–60 days) is applied to the 1000-hPa zonal winds over the WEP. In the SP type, the square of the MJO amplitude of these winds (Fig. 7) indicates that the MJO increases significantly in February (Fig. 7a), which is about one month before the enhancement of the HCA anomaly in the CEP and its further eastward propagation (see Fig. 5a). For the SU events, the MJO remains weak until about May 1 (Fig. 7b), which is again about one month prior to the eastward propagation of the HCA anomaly (see Fig. 5b). Therefore, it appears that the timing of when the MJO reaches an appreciable magnitude may be an important factor in determining the onset time of the warm event.

#### f. Statistical significance

The small sample size in each of the two categories of events (6 samples each) raises the issue of statistical significance of the results. Therefore, differences in the anomalies between the two categories are compared using the two-sample  $t$  test. Rather than testing all the

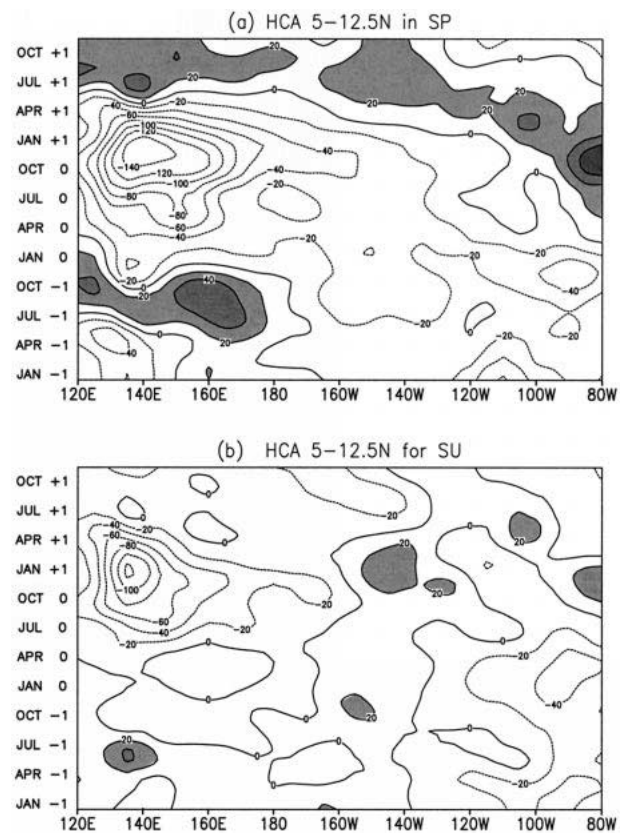


FIG. 6. Longitude–time section of HCAs from 0- to 400-m depth composites over  $5^{\circ}$ – $12.5^{\circ}\text{N}$  for (a) SP and (b) SU. Shaded areas indicate HCAs  $> 20 \text{ J m}^{-2}$ , unit:  $10^8 \text{ J m}^{-2}$ .

variables analyzed in this study, the two most crucial parameters are examined: the SSTA, based on which the classification of the two categories is made; and the wind stress, based on which the hypothesis for the initiation of the warm event is proposed.

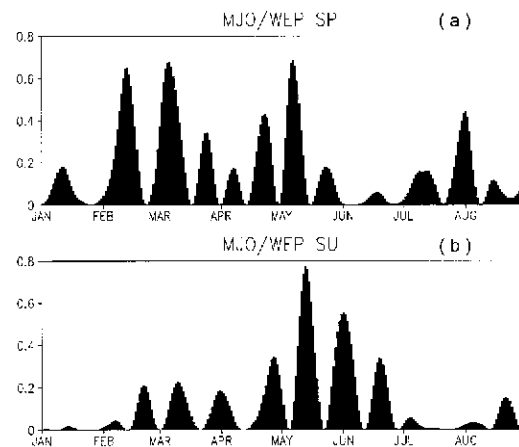


FIG. 7. Composite of the square of the MJO amplitude of the 1000-hPa zonal winds over the WEP for (a) SP and (b) SU events during the first eight months of year 0. Unit:  $\text{m}^2 \text{ s}^{-2}$ .

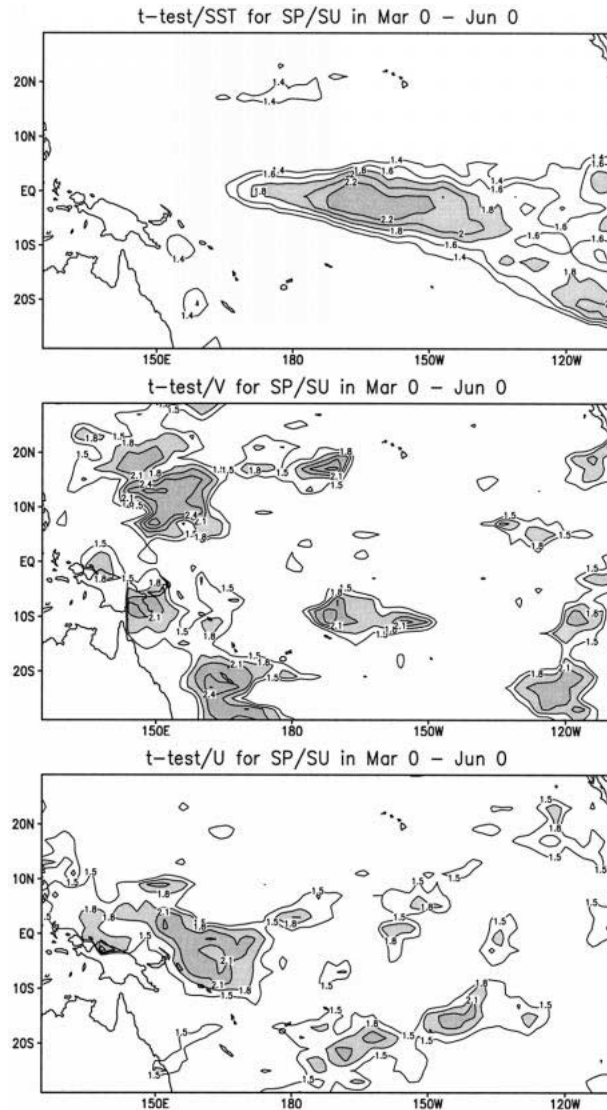


FIG. 8. The  $t$  value in the two-sample  $t$  test of the difference between SP and SU episodes during Mar 0 to Jun 0 for (a) SSTA, (b) meridional wind stress anomalies, (c) zonal wind stress anomalies. Shading indicates areas in which the  $t$  value exceeds the confidence level of 0.10.

As might be expected from Fig. 2, the most significant difference in SSTA between the SP and SU episodes during the transition period (March 0 and June 0) is in the Niño-3.4 region where the  $t$  values are very large ( $>2.2$ ; Fig. 8a). These values are significant above the 95% level. The  $t$  values exceeding the 90% significant level cover the entire tropical eastern Pacific. Therefore, the two categories of events can be considered to be independent, which is evident from the results presented.

During the same period when the wind stress shows a substantial difference (see Fig. 3), the  $t$ -test result shows that the meridional wind stresses in the north-eastern part of Australia and northwest Pacific are sig-

nificantly different between the SP and SU episodes (Fig. 8b). Note also that the significant differences include only the Australian monsoon and east Asian monsoon areas. In addition, the  $t$ -test results for the zonal wind stress (Fig. 8c) show significant differences in the WEP, which is the crucial area for the initiation of an El Niño event.

The tests presented here clearly demonstrate that despite the relatively small sample size, warm events of the ENSO cycle can indeed be divided into two general categories based on the onset time. Further, the physical hypothesis advanced in this study should be largely valid.

#### g. Summary

To summarize, the two types of events have similarities as well as differences. From the atmospheric perspective, both types have appreciable anomalous westerlies appearing over the WEP about three months prior to the onset time. In addition, the EAWM is strong in the winter before the EN year. Further, anomalous southerlies appear off the northeast coast of Australia one to two months prior to the onset time. When these southerly anomalies appear seems to determine the onset time. To some extent, the above features are consistent with the results described in previous studies that emphasized the roles of the variation in the South Pacific in the ENSO onset (Rasmusson and Carpenter 1982; Hackert and Hastenrath 1986; Kiladis and Diaz 1989; van Loon 1984; Van Loon and Shea 1985; Meehl 1987; Wang 1995).

In both types, positive SSTAs appear in the WEP about six months prior to the onset of the EN event, and then propagate eastward a few months later. The heat content of the upper ocean, however, varies differently in the two types. While these results suggest that these two types of EN events are different, such differences could simply be due to a shift in the SST background state. Indeed, Wang (1995) has suggested that the interdecadal variation of this background state can affect the onset location and sequence of the EN event, as to whether a South American coastal warming leads or follows a CEP warming. The question is whether this interdecadal variation can also modify the onset time of EN events.

To address this issue, the interdecadal variation of the Niño-3.4 SST is obtained using a 132-month (11-yr) running mean. The interdecadal component time series shows that the CEP SST experiences two cold states in the 1950s and 1970s and two warm states in the 1960s and 1980s–90s (Fig. 9). The increase in SST in the late 1970s corresponds to the results found by Nitta and Yamada (1989) and Wang (1995). Note, however, that the occurrence of the two types of EN episodes does not appear to have any relationship with the interdecadal variation. This can be further demonstrated by removing this interdecadal component from the original time se-

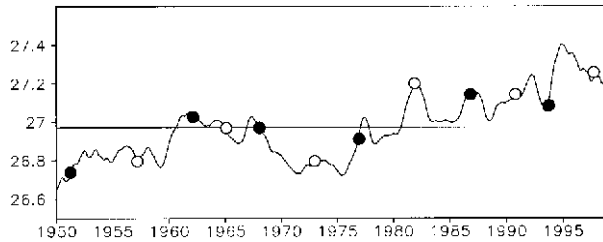


FIG. 9. The interdecadal variation of Niño-3.4 SST derived from a 132-month (11-yr) running mean for 1950–98. The dots and circles represent the onset time of the SU and SP EN events, respectively.

ries of Niño-3.4 SST. The composites of the SSTA (after removal of the interdecadal component<sup>1</sup>) for the two types of EN episodes (Fig. 10) are almost exactly the same as those shown in Fig. 2a. In other words, the difference in the onset time between these two types should be physical.

## 5. Relationship between equatorial westerly anomalies and various monsoon circulations

### a. The Indian monsoon region

Consistent with past studies, the analyses in this study show that westerly anomalies over the equatorial Pacific are strongly related to the occurrence of an EN event. The question then is to identify the physical processes responsible for the initial changes in the WEP wind field. Some studies (Barnett 1985; Meehl 1987; Yasunari 1990) have suggested that the westerly anomalies originate from the Indian summer monsoon. However, the evidence presented so far has not been conclusive.

To explore this problem further, the time–longitude section of the 1000-hPa zonal wind anomalies over the equatorial Pacific (5°S–5°N) for 1958–97 is examined (Fig. 11). Westerly anomalies always appear over the WEP before an EN event occurs. These anomalies may be traced back to the previous summer over the EIO. It appears that the WEP westerly anomalies are closely related to the Indian summer monsoon anomalies and seem to propagate slowly eastward. However, there exist many years in which westerly anomalies occurred in the summer over the EIO, but no eastward propagation occurred and no EN event developed in the following year, for example, 1958, 1960, 1970, 1973, 1978, 1980, 1984, 1989, 1990, and 1992. Further, even if the westerly anomalies originating from the Indian monsoon area did propagate eastward, they did not necessarily lead to an EN occurrence, for example, from 1970 to 1971, 1979 to 1980, 1989 to 1990, 1992 to 1993. These results, therefore, suggest that the westerly anomalies and their eastward propagation are only necessary conditions for

<sup>1</sup> This is calculated by subtracting the value of the 132-month (11-yr) running mean from that in the original time series.

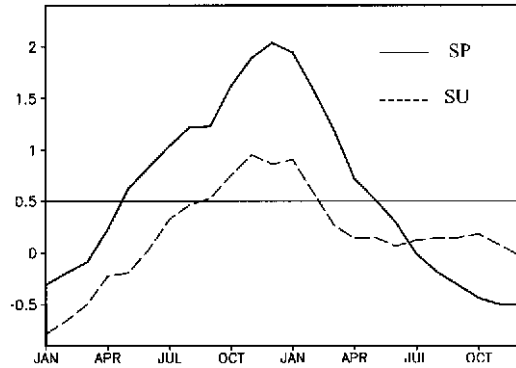


FIG. 10. As in Fig. 2a except after removal of the interdecadal component.

the development of EN episodes. This is consistent with the conclusion of McPhaden (1999).

Notice also from Fig. 10 that even for EN events, the eastward propagation of the westerly anomalies is generally not continuous. To study this question of propagation further, the 1000-hPa monthly mean zonal winds over the equatorial Indian and Pacific Oceans (5°S–5°N) are composited for the two types of EN episodes. The results (Fig. 12) suggest that the magnitude of the westerly anomalies for SP events is larger than that for the SU event. However, for both types, the westerly anomalies strengthen considerably east of 140°E. In addition, these anomalies, which apparently originate from the Indian Ocean, break off over the Maritime Continent (100°–120°E). The 850-hPa zonal winds also show similar features (not shown).

These results imply that the WEP westerly anomalies associated with EN events are influenced not only by the conditions over the Indian monsoon area. Some other factors must also be present. The analyses in section 4 suggest that east Asian and Australian monsoons may play an important role.

### b. The Asian–Australian monsoon region

To address this problem, the low-level circulations associated with these two monsoon systems are composited according to the different phases of the EN evolution: November –1 to January 0 as the antecedent condition, February 0 to April 0 as the occurrence phase of SP event, and May 0 to July 0 as that of the SU. For the SP event, in November –1 to January 0 (left upper panel in Fig. 13), the maximum westerly anomalies occur over the Maritime Continent. During this time, anomalous northerlies associated with a strong EAWM prevail over eastern China and the South China Sea. In the occurrence phase of the SP event (left middle panel), the strongest westerly anomalies have propagated to the WEP. Anomalous northerlies cover the entire western North Pacific, with one maximum directly north of the WEP westerly anomaly center. At the same time, noticeable anomalous southerlies are found over the north-

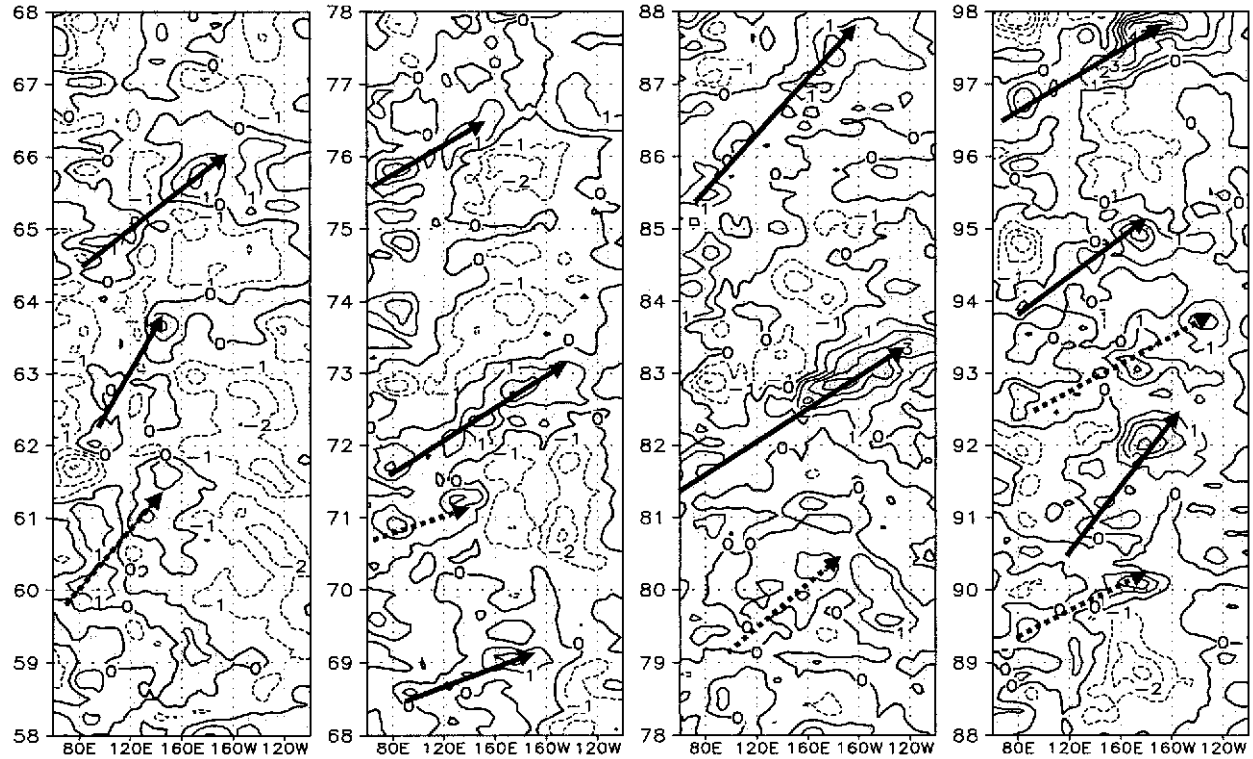


FIG. 11. Longitude–time section of 1000-hPa monthly mean zonal wind anomalies over the equatorial Pacific ( $5^{\circ}\text{S}$ – $5^{\circ}\text{N}$ ) for 1958–97. Shaded areas indicate westerly anomalies. The heavy arrow shows the propagating direction of the anomalies, with solid for the EN episodes and dotted for non-El Niño years.

east coast of Australia. These two anomalous meridional flows would thus produce strong convergence over the WEP, which then results in an enhancement of the anomalous westerlies. Such a meridional convergence persists into May 0 to July 0 (left lower panel), which may have contributed toward the continued development of the EN event.

For the SU event, in November  $-1$  to January 0 (right upper panel in Fig. 13), only weak westerly anomalies exist over Indonesia south of the equator. Similar to the SP events, anomalous northerlies are found over eastern China and the South China Sea. Notice, however, the strong meridional divergence along  $\sim 160^{\circ}\text{E}$ . In February 0 to April 0, the area of westerly anomalies move to the west Pacific warm pool where the meridional winds are generally southerly. No meridional convergence can be found over the WEP, which may be the reason why the westerly anomalies cannot strengthen, leading to a delay in the onset of the EN event. A convergent flow over the western Pacific warm pool finally occurs is May 0 to July 0, which corresponds to the onset phase of SU event.

It is clear from these results that the enhancement of westerly anomalies over the WEP is closely related to the meridional wind anomalies of the east Asian and the Australian monsoons. Strengthening of WEP westerlies occurs only when anomalous northerlies from the

east Asian monsoon converge with anomalous southerlies from Australia.

## 6. Role of the Asian–Australian monsoon system

The results from the previous sections suggest that the following ingredients are related to the development of an EN event: strong Indian summer monsoon in the previous year, strong EAWM prior to the EN event, and southerly anomalies from the AM area during the EN year. In section 5, the occurrence of a strong Indian summer monsoon was shown to be a necessary but not sufficient condition. Here, the role of the east Asia–Australia monsoon system will be further explored.

The interannual variability of the east Asian winter monsoon and their association with EN episodes is first investigated. Since all EN episodes are associated with a strong east Asian winter monsoon, it is useful to have an index to represent the strength of this monsoon. The definition of Shi and Zhu (1996) is used. They defined an EAWM index  $MI_t$  (for year  $t$ ) as

$$MI_t = \frac{MI_t^* - \overline{MI}}{\sigma_{MI}},$$

where

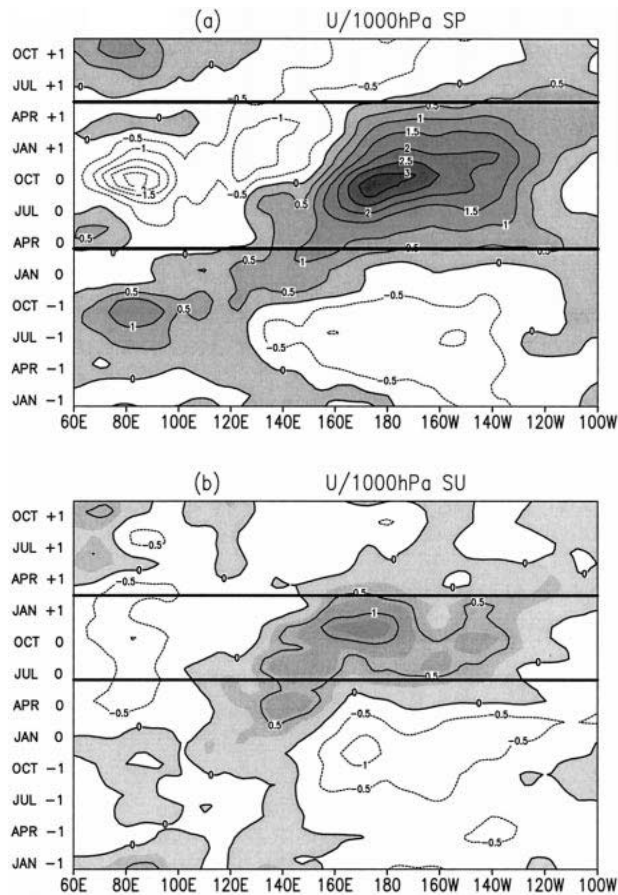


FIG. 12. Longitude–time section of composites of 1000-hPa monthly mean zonal wind anomalies over the equatorial area ( $5^{\circ}\text{S}$ – $5^{\circ}\text{N}$ ) for (a) SP and (b) SU events. Shaded areas indicate westerly anomalies. Thick horizontal lines indicate the mean start and end times of the EN event.

$$MI_i^* = \sum_{t=1}^7 (SLP_{11t}^* - SLP_{16t}^*),$$

where  $i = 1, 2, \dots, 7$  (latitude circle every  $5^{\circ}$  latitude from  $20^{\circ}$  to  $50^{\circ}\text{N}$ ),  $t = 1, 2, \dots, 7$  (year). The parameters  $\overline{MI}_i$ ,  $\sigma_{MI_i}$  represent the mean and standard deviation of  $MI_i^*$  over all years, respectively, and  $SLP_{11t}^*$ ,  $SLP_{16t}^*$  are standardized values in the  $t$ th year of the  $i$ th latitude along  $110^{\circ}$  and  $160^{\circ}\text{E}$ , respectively. Because in winter the SLP is generally high over land (along  $110^{\circ}\text{E}$ ) and low over the ocean (along  $160^{\circ}\text{E}$ ), this definition essentially gives a large-scale zonal pressure gradient. A large (small) value of  $MI_i$  therefore suggests a strong (weak) east–west gradient, which implies a strong (weak) winter monsoon. Notice that *winter* here means the average of December, January, and February.

The time series of the values of  $MI_i$  during 1950–97 (Fig. 14) suggests that of the 10 EN episodes, nine occurred when the EAWM was above normal in the previous winter except for the 1976–77 case, which agrees with the earlier results. However, above-normal winter

monsoons also occurred in years not followed by an EN event. Therefore a strong EAWM is again only a necessary condition for the occurrence of an EN event in the following year.

To study the role of the Australian monsoon anomaly in EN events, the meridional flow pattern of 4 yr (1960–61, 1970–71, 1977–78, and 1980–81) in which *both* the Indian summer monsoon in the previous summer and the EAWM winter monsoon were strong but *no* EN episode occurred in the following year are composited. These years will be referred to as NON years.

The composite patterns (Fig. 15) show that northerly anomalies dominate not only the western North Pacific but also off the northeastern coast of Australia during all the three phases. This means that when anomalous northerlies prevail over the Australian monsoon area, an EN episode will not occur even though the EAWM is strong. Such a meridional flow pattern does not produce convergence over the WEP, which is apparently necessary for the enhancement of westerly anomalies.

Based on above analysis, it may therefore be concluded that a strong southerly off northeastern Australia plays an essential role in the onset time of an EN episode. What is the mechanism for this? To address this question, the 850-hPa flow associated with anomalous circulation over the AM area are composited according to the different types of EN episodes. For the SP type (left panels in Fig. 16), in December –1 to January 0, cyclonic flow is found over northern Australia with a circulation off the northeastern coast of Australia, where the South Pacific Convergence Zone (SPCZ) is located. This pattern suggests a strong Australian summer monsoon. A similar situation is found in February 0 to March 0. In addition, an anticyclonic circulation appears over southeastern Australia. By April 0 to May 0, anticyclonic flow dominates over the entire Australian continent, which suggests that the Australian winter monsoon sets in earlier than normal. The flow pattern is similar in the southern summer (June 0 to July 0). Notice that throughout the entire eight months (December –1 to July 0), an anomalous cyclonic circulation is found off the northeast coast of Australia, which results in the southerly anomalies shown in Figs. 3 and 13. Therefore, it appears that a quasistationary cyclone over the SPCZ together with an earlier than normal onset of the Australian winter monsoon activity is essential for an EN episode to begin in April.

For the SU event (middle panels in Fig. 16), the cyclonic circulation and the monsoon trough associated with the Australian summer monsoon is confined over the continent during December –1 to January 0. An anomalous anticyclonic circulation replaces the climatological SPCZ off the east coast of Australia. In February 0 to March 0, the monsoon trough is oriented northwest–southeast so that northerly anomalies are found along the east coast. By April 0 to May 0, southerlies from southwestern Australia finally split the monsoon trough, with the eastern part migrating eastward

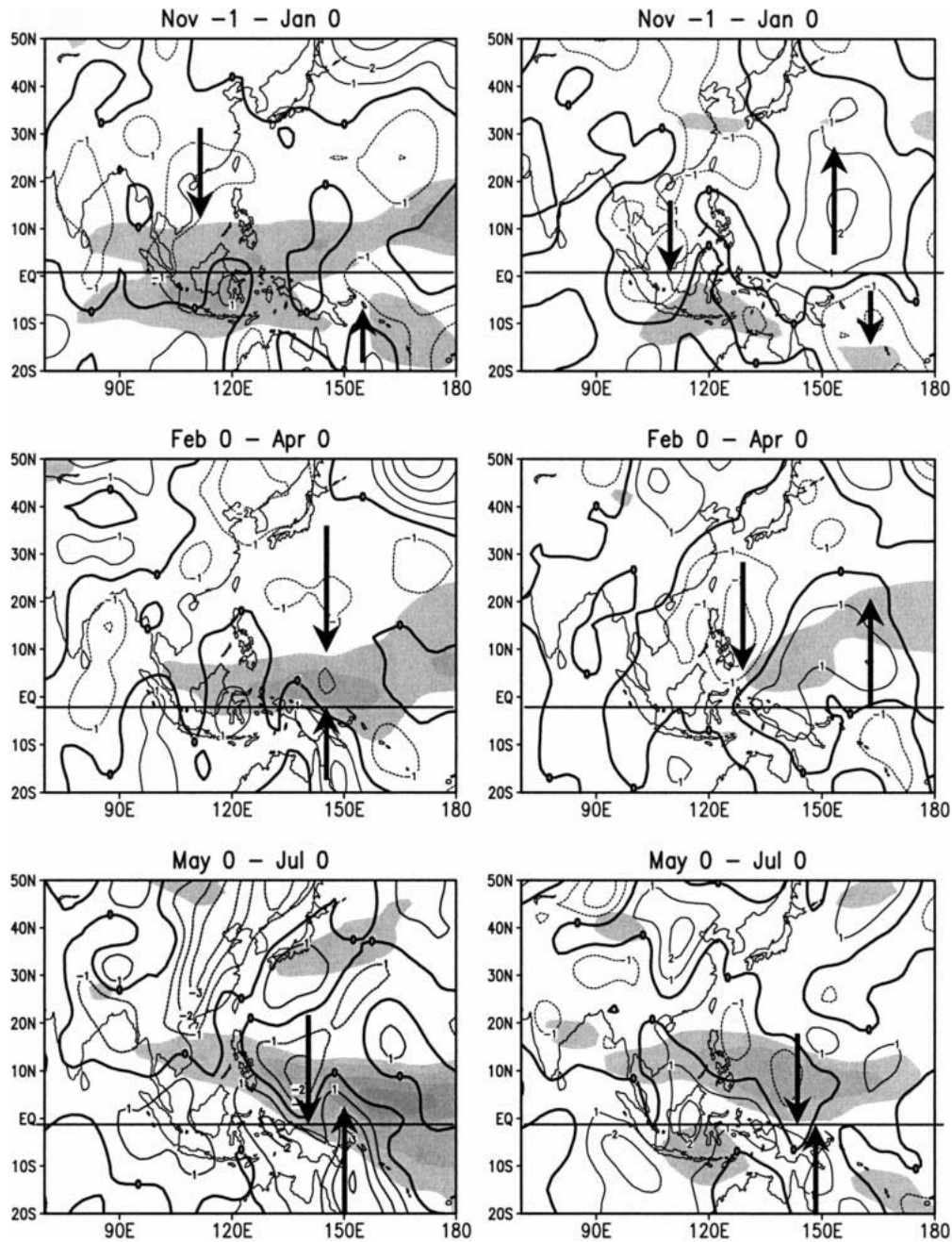


FIG. 13. Composite of 850-hPa meridional wind anomalies ( $\text{m s}^{-1}$ ) for (left) SP and (right) SU events in (top) Nov -1 to Jan 0, (middle) Feb 0 to Apr 0, and (bottom) May 0 to Jul 0. Shaded areas indicate zonal wind anomalies  $> 2.0 \text{ m s}^{-1}$ . The heavy solid arrows highlight the direction of meridional wind anomalies.

off the continent to the climatological SPCZ location. As a result, southerlies begin to appear off the northeastern coast of Australia. These anomalous southerlies are better established with the further development of the SPCZ in June 0 to July 0. Notice, however, that cyclonic anomalies still persist over the continent, which suggests a weaker-than-normal Australian winter monsoon.

In the NON type, the monsoon trough associated with

the Australian summer monsoon in December -1 to January 0 is split into two (right panels in Fig. 16), one part corresponding to the SPCZ and the other off the northwest coast. The continent is actually dominated by anticyclonic anomalies. This situation generally persists into May 0. By June 0 to July 0, the winter monsoon affects the southwestern part of the continent but a large cyclonic anomaly presides over the east coast of Australia. As a result, northerly anomalies are found off the east coast.

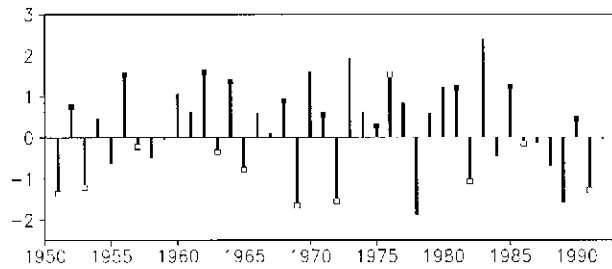


FIG. 14. Time series of the EAWM index (see definition in text) for 1950–51 to 1996–97. Here “winter” is the mean of Dec–Jan–Feb. Empty boxes indicate the EN years. Solid squares highlight the intensity of EAWM in the years prior to the EN episodes.

Thus, the evolution of the Australian monsoon (both winter and summer) system apparently determines whether and when southerly anomalies can develop off the east coast of Australia. A strong summer monsoon *and* an early (and perhaps strong) winter monsoon are essential for the early initiation of these anomalies. A weaker winter monsoon could delay the establishment of these anomalies while a weak summer monsoon does not allow the northward extension of the SPCZ off the eastern coast, which is necessary for the development of southerly anomalies. Some previous studies have pointed out that a warm event onset is associated with an active SPCZ (e.g., Kiladis and Diaz 1989; van Loon 1984; van Loon and Shea 1985; Meehl 1987). The results presented here further identifies the physical link between the two.

## 7. Summary and discussion

### a. Summary

Based on the first occurrence of a significant sea surface temperature anomaly (SSTA) over the central equatorial Pacific (the Niño-3.4 region), two types of El Niño events can be identified: the spring (SP) type in which the SSTA first exceeded  $0.5^{\circ}\text{C}$  in April or May; and the summer (SU) type in which the SSTA does not reach this threshold until July or August. A composite of the SSTAs suggests that the SP event is generally stronger and has a longer period in which the SSTA is above the threshold. The statistical significance tests presented here clearly demonstrate that despite the small sample size, warm events of the ENSO cycle can indeed be divided into two general categories based on the onset time.

The time evolution of the atmospheric conditions associated with these two types of El Niño event points to three important ingredients: a strong Indian summer monsoon in the year prior to the occurrence of the event, a strong east Asian monsoon during the winter immediately preceding the event, and a strong southerly from Australian monsoon during the El Niño year. The main difference between the two types is in the timing of occurrence of the westerly anomalies. For the SP (SU)

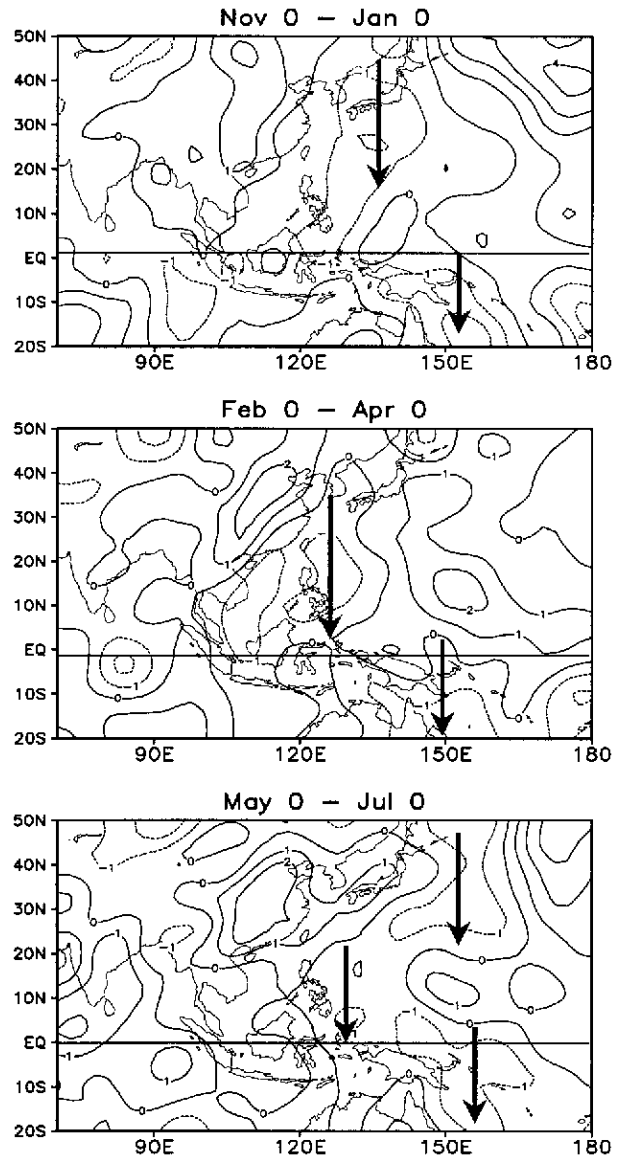


FIG. 15. As in Fig. 13 but for the composite of the meridional wind components for NON years.

event, westerly anomalies first appear over the western equatorial Pacific (WEP) in January (May). As the SST over the WEP peaks at around April, the anomalies associated with SP events are phase locked with the annual SST cycle so that these events have a larger SSTA amplitude. On the other hand, because the westerly anomalies associated with the SU event do not occur until after the SST has reached its maximum, they cannot produce significant warming over the WEP or the eastern equatorial Pacific.

When westerly anomalies can develop depends on the strength of the east Asia–Australia monsoon system. While a strong east Asia winter monsoon is found in both types of El Niño events, that for the SP episodes

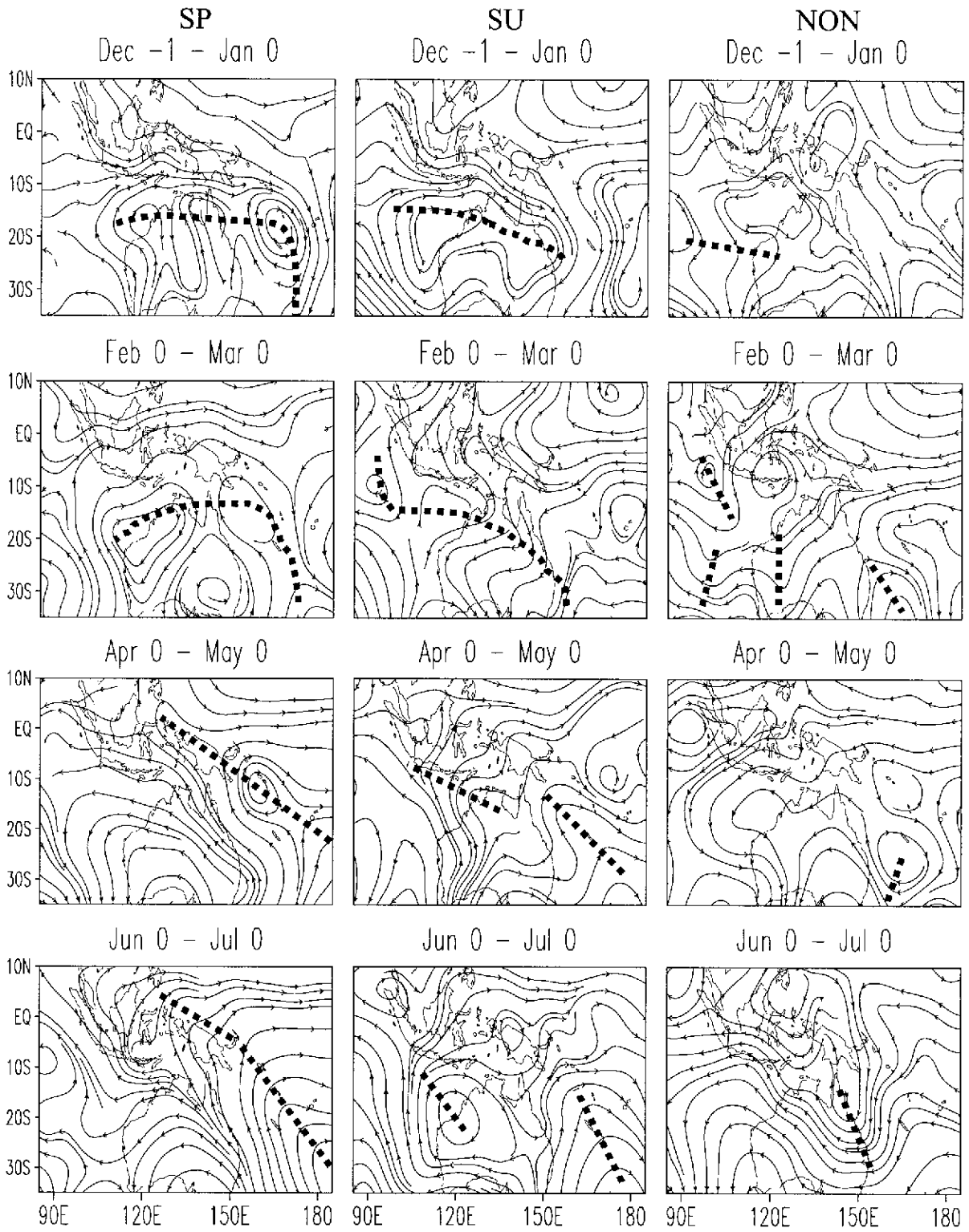


FIG. 16. Composite of 850-hPa flow anomalies mainly over Australia for (left) SP, (middle) SU, and (right) NON EN events.

appears to cover a larger part of the western North Pacific. The strong anomalous northerlies associated with this winter monsoon then converge with strong anomalous southerlies associated with the transition of Australia monsoon to produce enhanced westerly anomalies along the WEP early in the year. On the other hand, for SU episodes, meridional divergence is found in this region even around April of the El Niño year. Southerlies in the Southern Hemisphere do not appear until about May or June.

Of the three monsoon systems associated with both types of events, a strong Indian summer monsoon and a strong east Asian winter monsoon are found to be necessary conditions. Only when strong southerlies off the northeast coast of Australia are present (and can converge with northerlies from the Northern Hemisphere associated with a strong winter monsoon) can an El Niño event occur. The anomalous southerlies off the northeast of Australia appear substantially earlier than the onset time of El Niño, and are mainly controlled by the Australia monsoon activity and the anomalous cyclone over the SPCZ.

#### *b. Discussion*

The results of this study appear to have provided an answer to two questions related to the El Niño phenomenon: 1) what is the cause of the enhancement of the westerlies in the WEP, which is apparently responsible for the eastward propagation of warm water; and 2) why do some El Niño events occur in spring and some in summer?

For the first question, a number of hypotheses have been made that include the effects of the Southeast Asia winter monsoon (Lau et al. 1986; Li 1990), the Australian summer monsoon (Hackert and Hastenrath 1986), and the south Asian summer monsoon (Yasunari 1985, 1990; Meehl 1987). The current study clearly shows that all these monsoon components play important roles. Among these, the southerlies associated with the Australia monsoon appear to be crucial. If they occur earlier in the season, they can be in phase with the peak in the annual SST cycle in the WEP to trigger a larger ocean response and lead to an El Niño event onset in spring. On the other hand, a delayed occurrence of these southerlies beyond this peak will only result in a weak El Niño event onset in summer. If no anomalous southerlies appear, the El Niño event will not occur. These results are consistent with McPhaden's (1999) conclusion that the southerlies associated with the Southern Hemisphere cold surges strengthen the convective blow-ups in the WEP, westerly wind bursts, and, in some cases, ENSO event initiation. Notice, however, that the role of the Australian monsoons is predicated on a strong westerly anomaly over the equatorial Indian Ocean associated with the south Asian summer monsoon in the previous year, and a strong northerly anomaly from the east Asian winter monsoon over the east Asian coast.

Thus, it appears that more attention must be paid to the strength and timing of the Australian monsoons and how they couple with the Asian monsoon systems.

Although this study has addressed two key questions, a new issue appears, which is the factors that determine the time of occurrence of the southerly anomalies off the Australian coast. The analyses presented in this study suggest the seasonal transition of Australia monsoon and a persistent cyclone over the SPCZ as two important factors. The former is closely related to the cold surge activity associated with Australian monsoon systems. It is likely that such Southern Hemisphere cold surges are an actual manifestation of the southerlies east of Australia as noted by Meehl et al. (1996). For the latter, since the cyclone always appears before the El Niño onset, it is similar to the Australian onset cyclone discussed by Wang (1995). Furthermore, because the southerly anomalies apparently develop *prior to* the El Niño onset, they are likely a cause rather than an effect. On the other hand, the subsequent evolution of the cyclone and the anomalous southerlies and westerlies in the CEP may involve an air-sea interaction feedback.

Another issue is the contribution of the MJO. In addition to its relationship with westerly wind bursts, Matthews et al. (1996) have found that it can modulate the strength of the SPCZ. This study has shown that the latter is an important component in the onset time of the warm episode. Therefore, more investigation would be necessary to establish the role of the MJO and its relationship with the systems in the Southern Hemisphere. This will be the topic of a future study.

*Acknowledgments.* The authors would like to thank NCEP for providing the reanalysis data and the global SST data, Scripps Institution of Oceanography for providing the ocean heat content data, and The Florida State University for providing the pseudostress data. Thanks are extended to Ms. M.-H. Wang for her preliminary work on this topic. Part of the work of the second author was completed while he was a Croucher Foundation Senior Research Fellow and on sabbatical at the University of Hawaii (UH). He would like to thank Prof. Bin Wang for supporting his visit to UH. Prof. Wang also provided some constructive comments on an earlier version of the manuscript. The comments and suggestions offered by the two anonymous reviewers contributed to considerable improvements of the paper.

This research is sponsored by the City University of Hong Kong research Grant 9360017, and the Research Grants Council of Hong Kong Grant 9050249. Work of the first author is also partly sponsored by the National Natural Science Foundation of China Grant 49705062.

#### REFERENCES

- Angell, J. K., 1981: Comparison of variations in atmospheric quantities with sea surface temperature variations in the equatorial eastern Pacific. *Mon. Wea. Rev.*, **109**, 230–243.

- Barnett, T. P., 1985: Variations in near global sea level pressure. *J. Atmos. Sci.*, **42**, 478–501.
- , 1991: The interaction of multiple time scales in the tropical climate system. *J. Climate*, **4**, 269–285.
- Battisti, D. S., 1988: Dynamics and thermodynamics of a warming event in a coupled tropical atmosphere–ocean model. *J. Atmos. Sci.*, **45**, 2889–2919.
- Enfield, D. B., and L. S. Cid, 1991: Low-frequency changes in El Niño–Southern Oscillation. *J. Climate*, **4**, 1137–1146.
- Fu, C., H. F. Diaz, and J. O. Fletcher, 1986: Characteristics of the response of sea surface temperature in the central Pacific associated with warm episodes of the Southern Oscillation. *Mon. Wea. Rev.*, **114**, 1716–1738.
- Gill, A. E., and E. M. Rasmusson, 1983: The 1982–1983 climate anomaly in the equatorial Pacific. *Nature*, **306**, 229–234.
- Hackert, E. C., and S. Hastenrath, 1986: Mechanisms of Java rainfall anomalies. *Mon. Wea. Rev.*, **114**, 745–757.
- Hirst, A. C., 1986: Unstable and damped equatorial modes in simple coupled ocean–atmosphere models. *J. Atmos. Sci.*, **43**, 606–630.
- Holland, G. J., 1986: Interannual variability of the Australian summer monsoon at Darwin: 1952–1982. *Mon. Wea. Rev.*, **114**, 594–604.
- Ju, J., and J. Slingo, 1995: The Asian summer monsoon and ENSO. *Quart. J. Roy. Meteor. Soc.*, **121**, 1133–121.
- Kiladis, G. N., and H. F. Diaz, 1989: Global climatic anomalies associated with extremes in Southern Oscillation. *J. Climate*, **2**, 1069–1090.
- Lau, K. M., and P. H. Chan, 1986: Aspects of the 40–50 day oscillation during the northern summer as inferred from outgoing longwave radiation. *Mon. Wea. Rev.*, **114**, 1354–1367.
- , and P. J. Sheu, 1988: Annual cycle, quasi-biennial oscillation, and Southern Oscillation in global precipitation. *J. Geophys. Res.*, **93**, 10 975–10 988.
- , and S. Yang, 1996: The Asian monsoon and the predictability of the tropical ocean–atmosphere system. *Quart. J. Roy. Meteor. Soc.*, **122**, 945–957.
- Li, C., 1990: Interaction between anomalous winter monsoon in East Asian and El Niño events. *Adv. Atmos. Sci.*, **7**, 36–46.
- Madden, R. A., and P. R. Julian, 1972: Description of global-scale circulation cells in the tropics with a 40–50 day period. *J. Atmos. Sci.*, **29**, 1109–1123.
- , and —, 1994: Observations of the 40–50-day tropical oscillation—A review. *Mon. Wea. Rev.*, **122**, 814–837.
- Matthews, A. J., B. J. Hoskins, J. M. Slingo, and M. Blackburn, 1996: Development of convection along the SPCZ within a Madden–Julian oscillation. *Quart. J. Roy. Meteor. Soc.*, **122**, 669–688.
- McPhaden, M., 1999: Genesis and evolution of the 1997–98 El Niño. *Science*, **283**, 950–954.
- Meehl, G. A., 1987: The annual cycle and interannual variability in the tropical Pacific and Indian Ocean region. *Mon. Wea. Rev.*, **115**, 27–50.
- , 1997: The South Asian monsoon and the tropospheric biennial oscillation. *J. Climate*, **10**, 1921–1943.
- , G. N. Kiladis, K. M. Weickmann, M. Wheeler, D. S. Gutzler, and G. P. Compo, 1996: Modulation of equatorial subseasonal convective episodes by tropical–extratropical interaction in the Indian and Pacific Ocean regions. *J. Geophys. Res.*, **101**, 15 033–15 049.
- Nicholls, N., 1984: Predicting Indian monsoon rainfall from sea-surface temperature in the Indonesia–north Australia area. *Nature*, **307**, 576–577.
- , 1989: Sea surface temperatures and Australian winter rainfall. *J. Climate*, **2**, 965–973.
- Nitta, T., and S. Yamada, 1989: Recent warming of tropical surface temperature and its relationship to the Northern Hemisphere circulation. *J. Meteor. Soc. Japan*, **67**, 375–383.
- Philander, S. G., 1985: El Niño and La Niña. *J. Atmos. Sci.*, **42**, 2652–2662.
- Quinn, W. H., and V. T. Neal, 1987: El Niño occurrences over the past four and a half centuries. *J. Geophys. Res.*, **92**, 14 449–14 461.
- Rasmusson, E. M., and T. H. Carpenter, 1982: Variations in tropical sea surface temperature and surface wind fields associated with the Southern Oscillation/El Niño. *Mon. Wea. Rev.*, **110**, 354–384.
- , and —, 1983: The relation between eastern equatorial Pacific sea surface temperature and rainfall over Indian and Sri Lanka. *Mon. Wea. Rev.*, **111**, 517–528.
- Reynolds, R. W., and T. M. Smith, 1994: Improved global sea surface temperature analyses using optimum interpolation. *J. Climate*, **7**, 929–948.
- Shi, N., and Q. Zhu, 1996: An abrupt change in the intensity of the East Asian summer monsoon index and its relationship with temperature and precipitation over East China. *Int. J. Climatol.*, **16**, 757–764.
- Shukla, J., and D. Paolino, 1983: The Southern Oscillation and the long-range forecasting of monsoon rainfall over India. *Mon. Wea. Rev.*, **111**, 1830–1837.
- Slingo, J. M., D. P. Rowell, K. R. Sperber, and F. Nortley, 1999: On the predictability of the interannual behaviour of the Madden–Julian oscillation and its relationship with El Niño. *Quart. J. Roy. Meteor. Soc.*, **125**, 583–609.
- Soman, J. K., and J. Slingo, 1997: Sensitivity of Asian summer monsoon to aspects of sea surface temperature anomalies in the tropical Pacific Ocean. *Quart. J. Roy. Meteor. Soc.*, **123**, 309–336.
- Suarez, M. J., and P. S. Schopf, 1988: A delayed action oscillator for ENSO. *J. Atmos. Sci.*, **45**, 3283–3287.
- Tomita, T., and T. Yasunari, 1996: Role of the northeast winter monsoon on the biennial oscillation of the ENSO/monsoon system. *J. Meteor. Soc. Japan*, **74**, 399–413.
- van Loon, H., 1984: The Southern Oscillation. Part III: Associations with the trades and with the trough in the westerlies of the South Pacific Ocean. *Mon. Wea. Rev.*, **112**, 947–954.
- , and D. J. Shea, 1985: The South Oscillation. Part IV: The precursors south of 15°S to the extremes of the oscillation. *Mon. Wea. Rev.*, **113**, 2063–2074.
- Wang, B., 1995: Interdecadal changes in El Niño onset in the last four decades. *J. Climate*, **8**, 267–285.
- Wang, S., 1992: Reconstruction of El Niño event chronology for the last 600-year period (in Chinese). *Acta Meteor. Sin.*, **6**, 47–57.
- Webster, P. J., and S. Yang, 1992: Monsoon and ENSO: Selectively interactive system. *Quart. J. Roy. Meteor. Soc.*, **118**, 877–926.
- Wyrski, K., 1975: El Niño—The dynamic response of the equatorial Pacific Ocean to atmospheric forcing. *J. Phys. Oceanogr.*, **5**, 572–584.
- Xu, J. J., Q. G. Zhu, and Z. B. Sun, 1998a: Interrelation between East-Asian winter monsoon and Indian/Pacific SST with the interdecadal variation. *Acta Meteor. Sin.*, **12**, 275–287.
- , —, and T. H. Zhou, 1998b: Monsoon circulation related to ENSO phase-locking. *Adv. Atmos. Sci.*, **15**, 267–276.
- Yasunari, T., 1985: Zonally propagating modes of the global east-west circulation associated with the Southern Oscillation. *J. Meteor. Soc. Japan*, **63**, 1013–1029.
- , 1990: Impact of Indian monsoon on the coupled atmosphere/ocean system in the tropical Pacific. *Meteor. Atmos. Phys.*, **44**, 29–41.